

# Classification of Fecal Contamination on Leafy Greens by Hyperspectral Imaging

Chun-Chieh Yang<sup>1</sup>, Won Jun<sup>1</sup>, Moon S. Kim<sup>1</sup>, Kuanglin Chao<sup>1</sup>, Sukwon Kang<sup>2</sup>, Diane E. Chan<sup>1</sup>, Alan Lefcourt<sup>1</sup>

<sup>1</sup>Environmental Microbial and Food Safety Laboratory, Animal and Natural Resources Institute, Agricultural Research Service, United States Department of Agriculture  
10300 Baltimore Ave, Beltsville, MD 20705

<sup>2</sup>National Academy of Agricultural Science, Rural Development Administration,  
Suwon 441-100, Korea

## ABSTRACT

This paper reported the development of hyperspectral fluorescence imaging system using ultraviolet-A excitation (320-400 nm) for detection of bovine fecal contaminants on the abaxial and adaxial surfaces of romaine lettuce and baby spinach leaves. Six spots of fecal contamination were applied to each of 40 lettuce and 40 spinach leaves. In this study, the wavebands at 666 nm and 680 nm were selected by the correlation analysis. The two-band ratio, 666 nm / 680 nm, of fluorescence intensity was used to differentiate the contaminated spots from uncontaminated leaf area. The proposed method could accurately detect all of the contaminated spots.

**Keywords:** Hyperspectral imaging, multispectral imaging, fluorescence, bovine fecal detection, food safety

## 1. INTRODUCTION

According to the United States Centers for Disease Control and Prevention (CDC), the number of foodborne illness outbreaks related to consumption of fresh produce occurring annually is increasing. Because animal fecal matter has the potential to introduce human pathogens to fresh produce<sup>1</sup>, vegetable crops grown in fields enriched with manure or in proximity to wildlife/livestock are drawing concerns due to the potential risk of contamination. Consumption of fresh leafy greens, such as lettuce, alfalfa, spinach, and sprouts, contaminated by fecal matter can cause human infection<sup>2</sup> and lead to foodborne illness outbreaks

Several *E. coli* O157:H7 outbreaks associated with romaine lettuce and spinach were reported recently<sup>3, 4</sup>. Such contamination may originate from irrigation water contaminated with wild pig feces<sup>2, 5</sup>. Foodborne illness outbreaks spurred several food safety initiatives to better protect public health from pathogens associated with fresh produce<sup>6, 7</sup>. Automatic inspection of fresh produce with fast and accurate detection of bovine fecal contamination on fresh produce will be helpful and essential for food processing industry.

Hyperspectral imaging technique has been applied to food safety and quality applications such as the detection of defects and fecal contamination on apples, cantaloupes, strawberries, and other fresh produce, and the detection of microbial contamination such as bacterial biofilms on food processing<sup>8, 9, 10</sup>. Among these techniques, fluorescence imaging has demonstrated promising detection results for spots of diluted fecal contamination on apples, with minimal false positives. The major contaminant constituents that allow detection of feces using fluorescence techniques are suggested to be chlorophyll a and its byproducts<sup>11</sup>.

Therefore, the primary object of this study was to use a hyperspectral fluorescence imaging system to determine multispectral wavebands for detection of bovine fecal matter on leafy green vegetables such as romaine lettuce and baby spinach. The main goal was to develop an algorithm to detect all of the fecal contamination spots for public health

concern while correctly identifying the uncontaminated leaf surfaces using selected multispectral wavebands for economic concern.

## 2. MATERIALS AND METHODS

To prepare leafy greens and dairy manure contamination materials, heads of romaine lettuce (*Lactuca sativa*) and loose baby spinach leaves (*Spinacia oleracea* L.) were obtained from a local market. Two to three leaves taken from each head of lettuce and each spinach leaf were washed using water for approximately 30 seconds. Fresh feces from Holstein cows were collected from the Dairy Operations Unit, Beltsville Area Research Center, Agricultural Research Service, United States Department of Agriculture. Collected feces were stored at -20 °C prior to the experiment. Fecal contamination was applied to 40 leaves of romaine lettuce and 40 spinach leaves, with 20 on adaxial surfaces and 20 on the abaxial surfaces for each type. Six fecal spots, each of 5-mm diameter, were applied to each lettuce and baby spinach leaf surface using a spatula. The leaves were placed on a tray of a non-fluorescent black cloth to simplify the study. The preliminary study showed that the highest difference of fluorescence intensity between objects and background of black cloth was observed at the waveband at 692 nm. Thus, this waveband was used to distinguish the object (leaf surface or fecal contamination) from the background (black cloth) in each image.

In this study, the hyperspectral line-scan imaging system was developed with an electron-multiplying-charge-coupled-device (EMCCD) camera, an imaging spectrograph, lenses, a pair of ultraviolet (UV)-A lights at 365 nm providing near-uniform illumination to the linear field of view (FOV), as shown in Figure 1. The EMCCD camera could acquire high-resolution images in high speed under low illumination environment, which is essential for scanning food product in high speed processing line. The spectrograph dispensed light to form a spectrum for each pixel along the linear field of view as line-scanning. When certain wavebands were selected for application, the hyperspectral imaging system could acquire multispectral images without the need for cross-system calibration while significantly increasing the image acquisition speed. A motorized table was used to move samples at a 0.5-mm interval to simulate line scanning in the real-world food processing line. Each line-scan image contained spectral data along one axis and spatial data along another axis. The original line-scan image size of 500 (spectral) × 400 (spatial) pixels was reduced by binning both the spectral and spatial dimensions by two, to reduce the image size to 250 × 200 pixels. From preliminary trial-and-error study to discard wavebands containing little information, only 60 channels ranging from 421 nm to 700 nm with an approximate 4.8 nm interval were used in this study. Thus, the line-scan images were further reduced to 60 × 200 pixels for analysis.

Figure 2 showed the emission spectra of fluorescence from 416 nm to 700 nm for leaf veins, inter-vein leaf surfaces and fecal contamination spots for adaxial and abaxial surfaces of romaine lettuce and baby spinach, respectively. Both the romaine lettuce and baby spinach leaves showed emission maxima between about 660 and 690 nm, related to the intensity of chlorophyll a emissions. When the leaves are exposed to UV-A excitation, UV-absorbing materials such as flavin, carotene, and phenolic compounds emit blue and green fluorescence<sup>12</sup> while chlorophyll a emits red and far red fluorescence<sup>13</sup>. In this spectral range, abaxial surfaces of leaves exhibited higher fluorescence emissions than adaxial surfaces of leaves did, due to higher scattering caused by more intercellular air spaces and less active photosynthesis in the abaxial surfaces<sup>14</sup>. The emission peak for the fecal contamination spots showed a shift toward the shorter waveband, called blue shift, comparing to the peaks for leafy greens area. Although the emission peaks for vein, inter-vein, and dairy manure were distinguishable from one another, they were not reliable and the difference among them were not unique, particularly for the adaxial surface of baby spinach, which indicated that a single waveband may not be sufficient for the detection of bovine fecal contamination on the leaf surfaces. The ratio of fluorescence intensity from two wavebands should be more appropriate to detect fecal contamination on leafy greens because, comparing to the intensity at a single waveband, the ratio of intensities from two wavebands could be less susceptible to relative intensity response and heterogeneous lighting resource.

After obtaining images, the correlation analysis was used to determine optimal waveband pairs for detection of fecal contamination spots. Spectra were extracted manually from uncontaminated leaf areas and within fecal contamination spots on the leaves. The spectral data were analyzed by the ratio of the fluorescence intensities measured at two different wavebands for all possible two-waveband combinations. The correlation coefficients between the two-band ratio of fluorescence and the binary output for each pixel, 1 for contaminated spot and -1 for leaf surface were calculated. Two wavebands for the ratio with the coefficient closest to 1 or -1 i.e., highest correlation between the ratio of fluorescence

intensities and the condition of the pixel, would be selected for fecal detection. However, the preliminary studies showed that the coefficients might range from 1 to -0.5 and none case showed any coefficient close to -1. Thus, the ratio presenting the coefficient closest to 1 would be selected in this study.

### 3. RESULTS AND DISCUSSION

Figure 3 showed the contour maps of correlation coefficients between the band-ratio of fluorescence and the binary output of 1 (contamination spot) or -1 (leaf surface) for romaine lettuce and baby spinach, respectively. The result showed that, for both fresh produces, the coefficient closest to 1 was obtained from the ratio of 666 nm over 680 nm, 0.98 for romaine lettuce and 0.96 for baby spinach. Therefore, the wavebands of 666 nm and 680 nm were selected for fecal contamination detection. The primary reason why the ratio of fluorescence intensities from the 666-nm and 680-nm wavebands were because of their correspondence to fluorescence emission peaks for fecal matter and chlorophyll a, since leafy green vegetables have relatively high chlorophyll content compared to the chlorophyll content of fecal contamination spots. This waveband selection also matched the spectra in Figure 2. The result also indicated the benefit using the ratio of fluorescence intensities which was better than the intensity from a single waveband for fecal contamination detection.

Figure 3 also showed that although there was another fluorescence emission peak at around 460 nm in Figure 2, the correlation coefficients varied from 0.3 to -0.3 while one of the pair of wavebands for calculating the ratio of intensities was close to this waveband. The correlation was so low that the fluorescence emission peak at this range of the spectrum could be discarded.

To further investigate the spectral ratio from these two wavebands, almost all of the fluorescence intensity for leaf area was lower than 0.45, and most of the intensity for fecal contamination was higher than this value. Thus, 0.45 was set as a single threshold to distinguish leaf area and fecal contamination. Moreover, because of shadow caused by uneven leaf surface, many individual pixels along leaf edge could be incorrectly identified as fecal contamination. To eliminate these false positive pixels, a  $3 \times 3$  filter was applied through all of the line-scan images.

Figure 4 showed the flowchart of the algorithm for the implementation of the selected wavebands and factors to the imaging system. After obtaining a line-scan image, the spatial image at the 692-nm waveband was used to create a mask. The mask was applied to the spatial images at the 666-nm and 680-nm wavebands to remove background of black cloth. The masked image at the 666-nm waveband was then divided by the one at the 680-nm waveband, pixel by pixel, to obtain the ratio image. The threshold of 0.45 was applied to the ratio image, giving any pixel whose ratio value was lower than the threshold the value of zero, and assigning the value of one to the rest pixels. The  $3 \times 3$  filter was then applied to the image to remove any false positive pixel. The final binary image presented the detection of fecal contamination on the leaf surface.

The developed algorithm was then applied to all 40 romaine lettuce and 40 baby spinach leaves, 20 of each species on adaxial side and the other 20 on the abaxial side, for evaluation. Figure 5 showed the example of the result. The result showed that the algorithm successfully detected all of the fecal contamination spots. Also, none of uncontaminated leaf surface was incorrectly marked. It showed that the hyperspectral imaging system with the developed multispectral imaging and detection algorithm could successfully detect the fecal contamination on the leaf surfaces and differentiate the contaminated fresh produce from the uncontaminated ones. The result also showed that the differences between two fresh produce (romaine lettuce and baby spinach), two leaf surface (adaxial and abaxial), and two leaf surface areas (inter-vein and vein) did not cause any difficulty to the detection of bovine fecal contamination. This benefit is essential for online application of the algorithm by saving computation and operation time and effort/

To eliminate the false positive pixels using the  $3 \times 3$  filter was important for the farmer's revenue concern. However, some contaminated spots may be missed by the filter. Thus, the original image and the final binary image were carefully compared and the pixels containing fecal contamination were manually counted for comparison. The result showed that 79% of pixels containing fecal matter in romaine lettuce leaves were correctly identified, and 63% of pixels containing fecal matter in baby spinach leaves were correctly identified. Although a portion of some fecal spots was missed due to image filtering, the spot itself was always correctly identified.

## 4. CONCLUSIONS

In this study, the hyperspectral fluorescence line-scan imaging system was developed for the detection of fecal contamination on the leaf surface of fresh produce. The research indicated that the wavebands of 666 nm and 680 nm should be selected, and the ratio of fluorescence intensities from these two wavebands should be used for bovine fecal contamination detection. The mask created by the waveband at the 692 nm could be used to distinguish the objects from the background before obtaining the ratio image. The threshold of 0.45 was applied to the ratio image to mark the pixels with fecal contamination, and the  $3 \times 3$  filter was then applied to eliminating false positive pixels. The final binary images showed that the algorithm could successfully detect all of fecal contamination spots on the adaxial and abaxial surfaces of romaine lettuce and baby spinach.

## 5. ACKNOWLEDGEMENTS

This research was partially supported by the Rural Development Administration, BioGreen 21 Program.

## 6. REFERENCES

1. Y. Kroupitski, D. Golberg, E. Belausov, R. Pinto, D. Swartzberg, D. Granot and S. Sela, "Internalization of *Salmonella enterica* in leaves is induced by light and involves chemotaxis and penetration through open stomata". *Applied and Environmental Microbiology*, **75**(19), 6076-6086. 2009.
2. J. Xicohtencatl-Cort and E. Sanchez Chacon. "Interaction of *Escherichia coli* O157:H7 with leafy green produce". *Journal of Food Protection*, **72**(7), 1531-1537. 2009.
3. FDA. *Questions & Answers: Taco Bell E. coli O157:H7 lettuce outbreak*. FDA, Washington, DC, 2006.
4. M. T. Brandl. Plant lesions promote the rapid multiplication of *Escherichia coli* O157:H7 on postharvest lettuce. *Applied and Environmental Microbiology*, **74**(17), 5285-5289. 2008.
5. G. L. Armstrong, J. Hollingsworth and J. G. Morris Jr. Emerging foodborne pathogens: *Escherichia coli* O157:H7 as a model of entry of a new pathogen into the food supply of the developed world. *Epidemiologic Reviews*, **18**(1), 29-51. 1996.
6. J. R. Gorny, H. Giclas, D. Gombas and K. Means. *Commodity Specific Food Safety Guidelines for the Lettuce and Leafy Greens Supply Chain*, International Fresh-cut Produce Association, Alexandria, VA, 2006.
7. D. M. Crohn and M. L. Bianchi. Research priorities for coordinating management of food safety and water quality. *Journal of Environmental Quality*, **37**(4), 1411-1418. 2008.
8. M. S. Kim, A. M. Lefcourt, Y. R. Chen and T. Yang. Automated detection of fecal contamination of apples based on multispectral fluorescence image fusion. *Journal of Food Engineering*, **71**(1), 85-91. 2005.
9. A. M. Vargas, M. S. Kim, Y. Tao and A. M. Lefcourt. Detection of fecal contamination on cantaloupes using hyperspectral fluorescence imagery. *Journal of Food Science*, **70**(8), 471-476. 2005.
10. W. Jun, M. S. Kim, K. Lee, P. Millner and K. Chao. Assessment of bacterial biofilm on stainless steel by hyperspectral fluorescence imaging. *Sensing and Instrumentation for Food Quality and Safety*, **3**(1), 41-48. 2009.
11. M. S. Kim, A. M. Lefcourt and Y. R. Chen. Optimal fluorescence excitation and emission bands for detection of fecal contamination. *Journal of Food Protection*, **66**(7), 1198-1207. 2003.

12. K. Chandrakuntal and N. Thomas. Fluorescence resonance energy transfer between polyphenolic compounds and riboflavin indicates a possible accessory photoreceptor function for some polyphenolic compounds. *Photochemistry Photobiology*, **82**(5), 1358-1364. 2006.
13. E. W. Chappelle, J. E. McMurtrey III and M. S. Kim. Identification of the pigment responsible for the blue fluorescence band in the laser induced fluorescence (LIF) spectra of green plants, and the potential use of this band in remotely estimating rates of photosynthesis, *Remote Sensing of Environment*, **36**(3), 213–218. 1991.
14. U. Schreiber and J. A. Berry. Heat-induced changes of chlorophyll fluorescence in intact leaves correlated with damage of the photosynthetic apparatus. *Planta* **136**(3), 233-238. 1977.

FIGURE 1. The hyperspectral fluorescence line-scan imaging system.

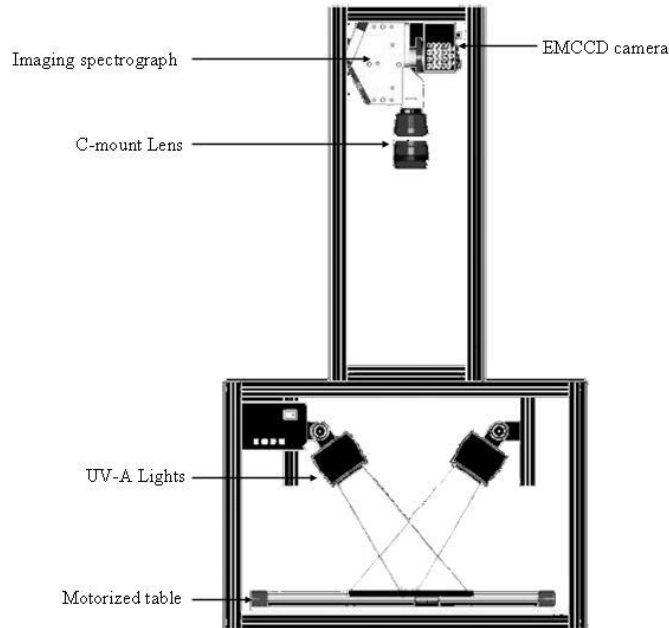


FIGURE 2. The spectra for (a) romaine lettuce at the adaxial surface, (b) romaine lettuce at the abaxial surface, (c) baby spinach at the adaxial surface, and (d) baby spinach at the abaxial surface.

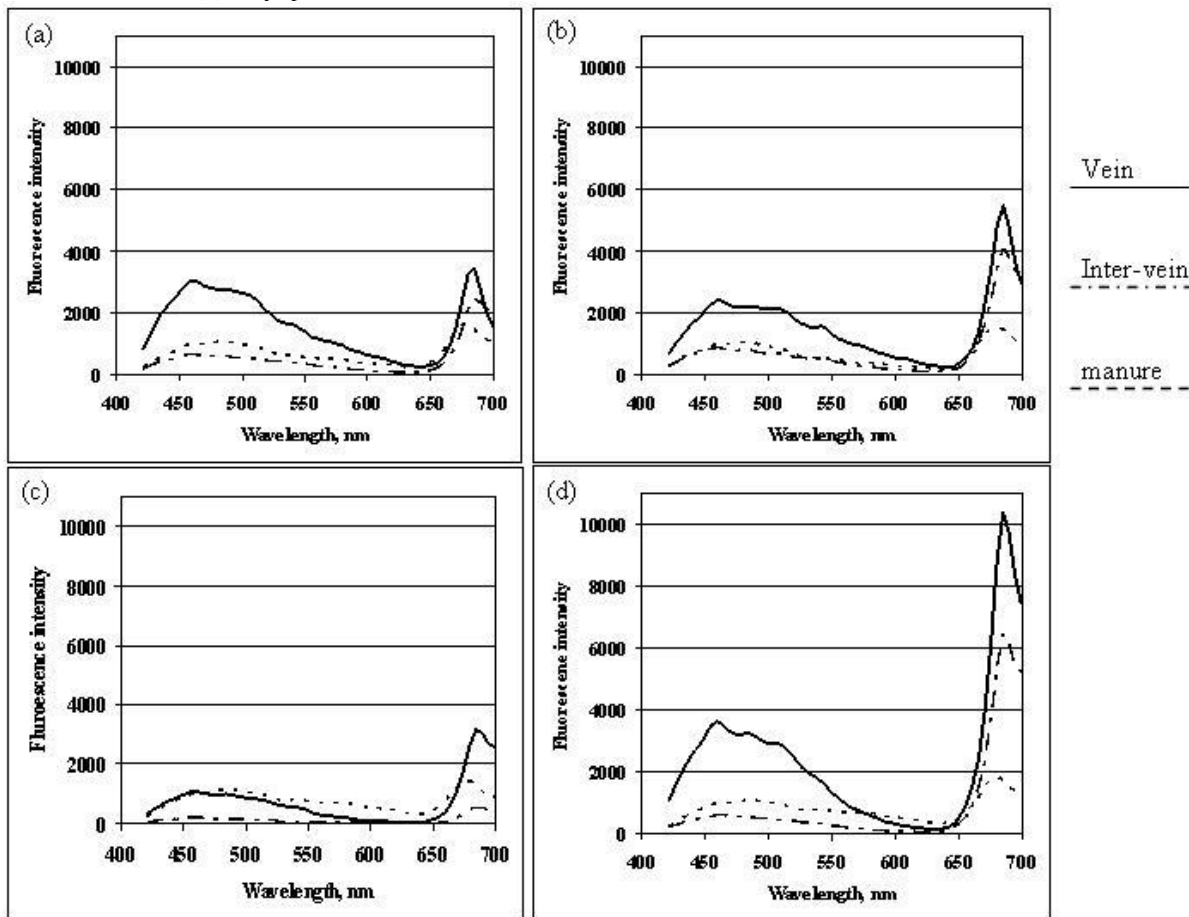


FIGURE 3. The contour maps for (a) romaine lettuce and (b) baby spinach.

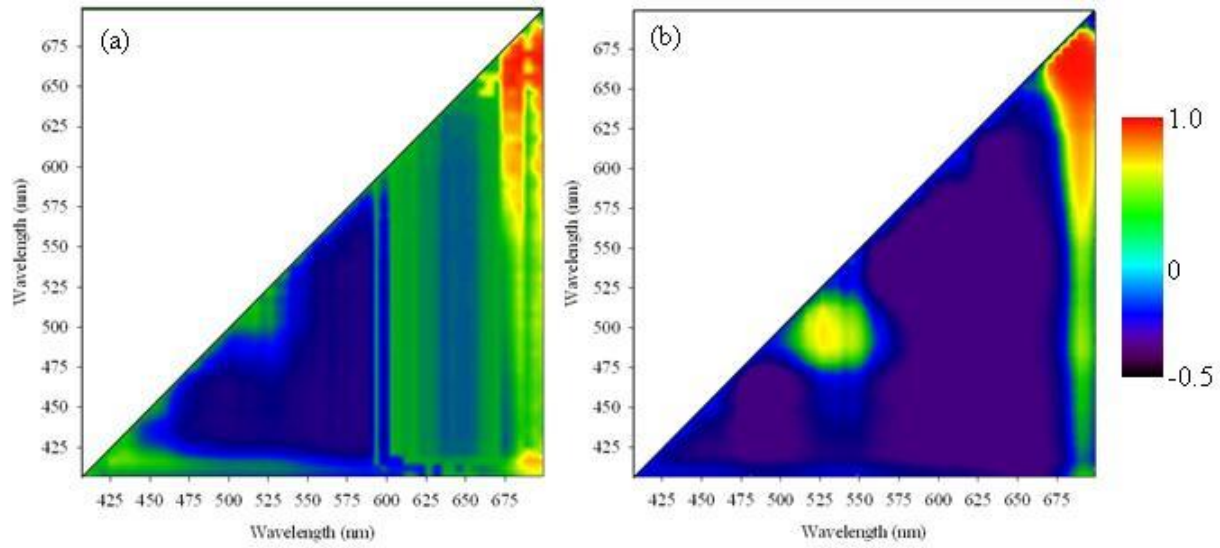


FIGURE 4. The flowchart for the image processing and fecal contamination detection algorithm.

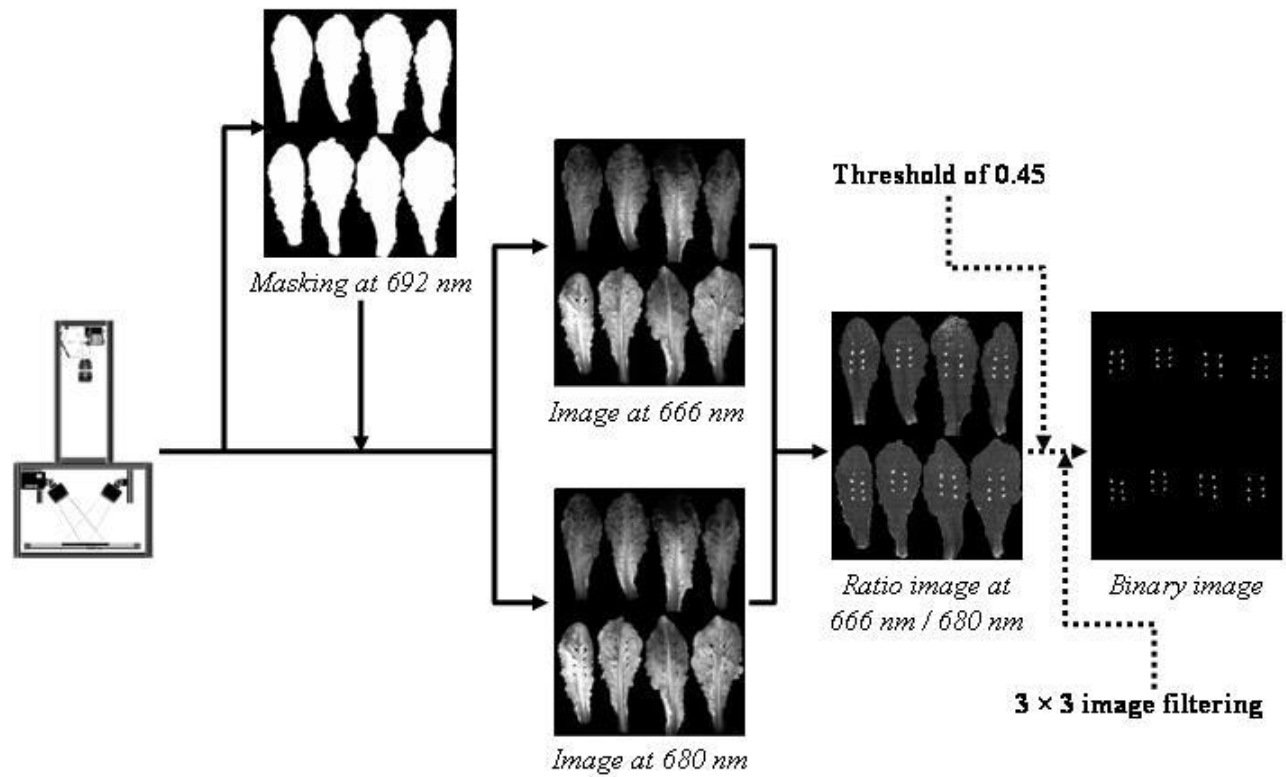


FIGURE 5. Example binary result images for the fecal contamination detection on the leafy surfaces.

